

Electronic Supplementary Information for

Poly(ionic liquid)-Wrapped Single-Walled Carbon Nanotubes for Sub-ppb Detection of CO₂

Yanxiang Li, Guanghui Li, Xuewen Wang, Zhiqiang Zhu, Hongwei Ma, Ting Zhang,* Jian Jin*

i-Lab, Suzhou Institute of Nano-tech and Nano-bionics, Chinese Academy of Sciences

Suzhou, 215123, China

1. Experimental section

Materials

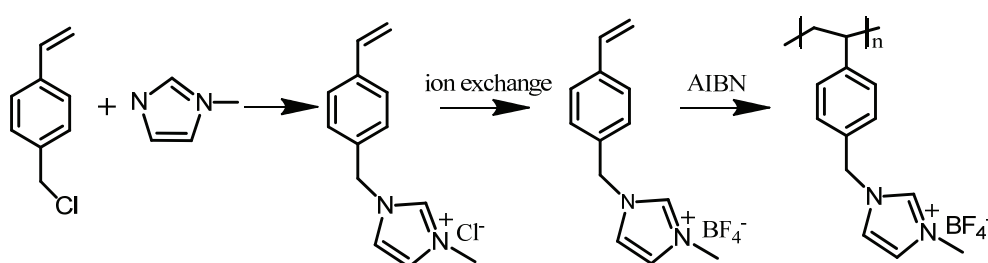
4-Vinylbenzyl chloride (90%), sodium tetrafluoroborate (NaBF₄), N-Methylimidazole (98%), 2,6-Di-tertbutyl-4-methylphenol (DBMP, 98%), α α' -Azobisisobutyronitrile (AIBN, 99%), anhydrous N’N-Dimethyl formamide (DMF) were purchased from Aldrich. High-purity single-walled carbon nanotubes (SWNTs) (>98 %) were purchased from Chengdu Organic Chemicals Co. Ltd., CAS. All other chemicals were analytical grade and used as received.

General Characterization

¹H NMR analysis was performed with a VARIAN 400 NMR spectrometer. Transmission electron microscope (TEM) images were recorded on a transmission electron microscope (TECNAI G2-F20) at an acceleration voltage of 200 kV. Scanning electron microscope (SEM) images were recorded on a Hitachi S-4800 microscope. Fourier transform infrared spectroscopy (FTIR) spectra were recorded on a Nicolet 6700 spectrometer by KBr disc technique. Quartz crystal microbalance (QCM) experiments were carried out on QCM resonators of Q-Sense E4 (Sweden). I-V characteristics were determined using Keithley 2602A source-meter. Tandem gel permeation chromatography/light scattering (GPC/LS) was done at room temperature using an SSI pump connected to Wyatt Optilab DSP and Wyatt DAWN EOS light scattering detectors with 0.02M LiBr in DMF as eluent at flow rate of 1.0 mL/min.

2. Synthesis of poly[1-(4-vinylbenzyl)-3-methylimidazolium tetrafluoroborate] (PIL) and characterization

The synthesis process of PIL is schematically shown in Scheme S1.



Scheme S1 Synthesis route of PIL

(a) *Synthesis of ionic liquid monomer: 1-(4-vinylbenzyl)-3-methylimidazolium tetrafluoroborate*

1-(4-vinylbenzyl)-3-methylimidazolium tetrafluoroborate (VBMIBF_4) was synthesized according to the literature.^[1] A detailed procedure can be described as follows: N-Methylimidazole (8.2 g), 4-vinylbenzyl chloride (15.2 g) and the inhibitor DBMP (0.10 g) were added into a dried flask. The reaction mixture was stirred at 40 °C under nitrogen for 24 h to yield a very viscous liquid, 1-(4-vinylbenzyl)-3-methylimidazole chloride (VBMICl). The compound was purified by washing with ethyl ether and dried overnight under vacuum at room temperature to give a transparent, viscous liquid. Then 1.22 g NaBF_4 in 15 ml dry acetone was added into 15 ml dry acetone containing 2.76 g VBMICl and 0.03 g DBMP. After stirred for 60 h, the solution was filtered, and the filtrate was evaporated under reduced pressure to yield a white and waxy solid. The crude product was further purified by washing with water and ethyl ether to obtain VBMIBF_4 .

^1H NMR (400 MHz, DMSO-d₆, δ) (Figure S1A): 3.85 (3H, s, N-CH₃), 5.40 (2H, s, Ph-CH₂-N-), 5.29 (1H, d, CH₂=CH-), 5.89 (1H, d, CH₂=CH-), 6.73 (1H, m, CH₂=CH-), 7.40 (2H, d, Ph), 7.51 (2H, d, Ph), 7.70 (2H, d, N-CH=CH-N), 9.17 (1H, s, N-CH-N).

(b) *Synthesis of PIL*

The above obtained VBMIBF_4 (1 g) and AIBN (10 mg) were dissolved in 2 ml DMF and stirred at 60 °C under nitrogen for 24 h. After this, the mixture was poured into methanol to yield precipitate. The precipitate was collected by filtration and washed with methanol thoroughly, then dried under vacuum at 50 °C to give yellowish solid, PIL.

^1H NMR (400 MHz, DMSO-d₆, δ) (Figure S1B): 0.6-2.0 (CH₃CH₂-Ph), 3.81(N-CH₃), 5.23 (Ph-CH₂-N-), 6.44, 7.01 (Ph), 7.60 (N-CH=CH-N), 9.05 (N-CH-N).

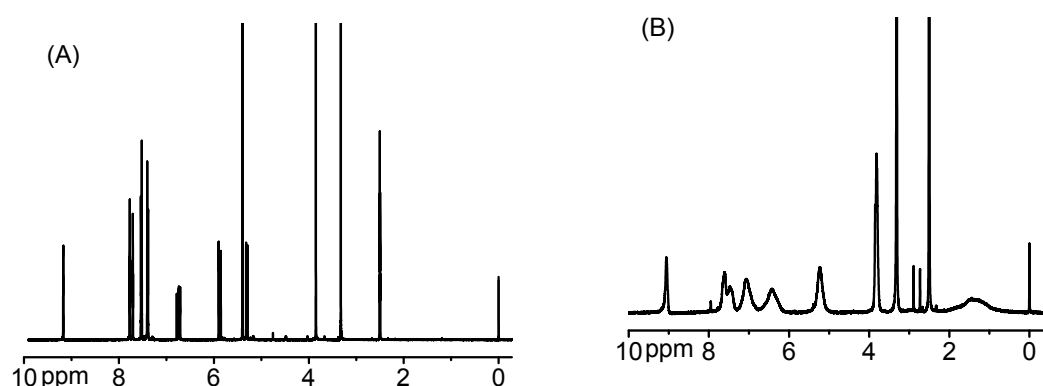


Figure S1 ¹H NMR spectra of (A) VBMIBF₄ and (B) PIL

Gel permeation chromatography/light scattering (GPC/LS) indicated that the as-synthesized PIL has molar mass of 44850 g/mol with polydispersity (Mw/Mn) of 1.3 (Figure S2).

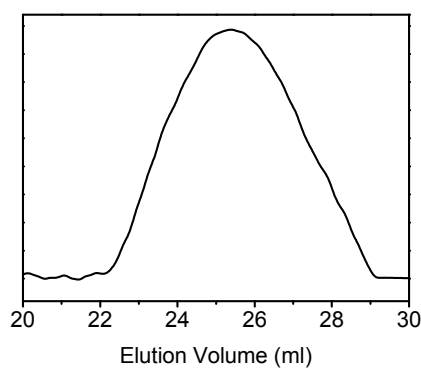


Figure S2 GPC trace of PIL in DMF eluent

3. QCM measurement of CO₂ adsorption capacity in PIL

To demonstrate the capacity of PIL in CO₂ adsorption, the as-synthesized PIL was spin-coated on a quartz crystal to explore the frequency response to CO₂ by means of Quartz Crystal Microbalance (QCM) measurement (Figure S3). In a typical experiment, the QCM cell with a PIL-coated crystal was purged with dry N₂ to establish a baseline frequency, then exposed to pure CO₂. The frequency decreased promptly upon exposed to CO₂ because of the increased mass resulting from CO₂ adsorption by PIL coating, and a stable frequency value was achieved (about 20 min). The cell was again purged with N₂ and the frequency recovered to its original baseline value (about 20 min). Three cycles of alternate exposure to CO₂ and N₂ didn't cause large changes in frequency shifts, indicating that the CO₂ response was reversible and reproducible. The CO₂ adsorption capacity was calculated to be 7.0 mg (CO₂)/g (PIL), consistent with that reported in

literature.^[2]

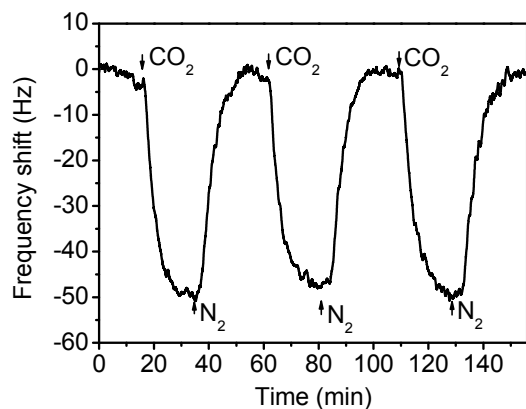


Figure S3 QCM response of PIL upon alternate exposure to pure CO₂ and N₂.

4. Preparation of PIL-wrapped SWNT suspension

1 mg PIL was dissolved in 20 µl DMF followed by the addition of 1 mg SWNTs. The mixture was ground for 30 min to obtain a black sticky gel. The gel was sonicated in 400 ml DMF for 5 h. A stable PIL/SWNTs dispersion was finally obtained by centrifuged at 5 000 rpm for 20 min.

5. Sensor device fabrication

The sensor arrays were patterned on a silicon substrate using standard photolithography as the procedure described earlier.^[3] A SiO₂ film (about 500 nm thick) was deposited on a highly doped silicon wafer via chemical vapor deposition as an insulating layer. Then the electrode area was defined using photolithography followed by sputtering a Cr/Au (20/200 nm, respectively) layer. Finally, the interdigitated electrodes with 10 µm gap were defined using lift-off techniques.

The PIL/SWNTs based CO₂ sensors are fabricated as follows: A 0.05 µL drop of the PIL/SWNTs suspension was deposited onto the electrode gap using a microsyringe. After evaporation of the solvent, PIL/SWNTs networks bridged each electrode as the conducting channel. The sensors were then dried at room temperature under vacuum for 48 h to remove any DMF residues present.

Gas sensing tests

For gas sensing test, the electrodes of the sensor arrays were wire-bonded using Au wire, and each sensor was connected in series with a load resistor. A quartz gas flow chamber with gas inlet and

outlet ports for gas flow through capped the sensor chip and sealed. An ultraviolet (UV, 365 nm) light source was installed above the chamber at a vertical distance about 20 cm. The total gas flow rate kept constant at 200 std. $\text{cm}^3 \text{ min}^{-1}$ regulated by mass flow controllers (MFCs, Sevenstar CS200, China). N_2 (purity: 99.999 %) was used as both carrier and diluting gas. Analyte gases with desired concentrations were generated by diluting CO_2 (purity: 99.999 %) with N_2 in gas sampling bags via MFCs. The accurate CO_2 concentration in the gas sampling bag was confirmed by gas chromatograph (GC) measurement (Zhejiang Fuli Analytical Instrument Co. Ltd., China) (Figure S4). A custom lab-view computer program was developed to continuously control and monitor the voltage of the circuit using Fieldpoint analog input and output modules (National Instruments, Austin, TX). In CO_2 sensing test, the sensors were first exposed to N_2 to obtain the stable baseline resistance, then switched to CO_2 with desired concentration, and then back to N_2 purge followed by short periods of UV light illumination to return the devices to their baseline resistances. All experiments were carried out at 24 °C. The sensitivity is defined as:

$$\frac{\Delta R}{R_0} \times 100\% = \frac{R_g - R_0}{R_0} \times 100\% \quad (1)$$

where R_0 is the baseline resistance in N_2 before exposure to CO_2 , and R_g is the resistance after exposed to different concentrations of CO_2 for 10 min.

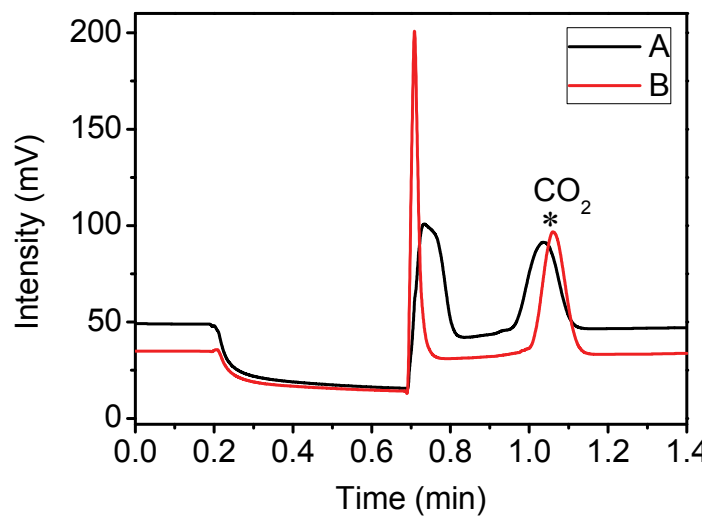


Figure S4 GC curves of CO_2 standard gas with 4 ppm concentration (A) and CO_2 in gas sampling bag as we made (B). The peak in the range of 0.9–1.2 min is associated to CO_2 , and the CO_2 concentration in the bag is calculated to be 4.07 ppm by comparing the integral area of the signal of CO_2 . This value is very close the expected 4 ppm CO_2 .

6. Sensor device fabrication

In order to understand the semiconducting type of the SWNTs, we compared the FET characteristics of SWNTs with and without PIL (Figure S5). As I_{SD} - V_G curve shown in Figure S5, the SWNTs and PIL/SWNTs based FET devices in our paper are both showing p-type semiconducting characteristics with small bandgap. For the SWNTs used in our paper, they are commercially purchased and mixed (metallic and semiconducting) tubes. Normally FET devices based on un-separated SWNTs network showed I_{on}/I_{off} ratios in the range of $10^{-1} \sim 10$, which is consistent with our SWNTs and PIL/SWNTs devices.

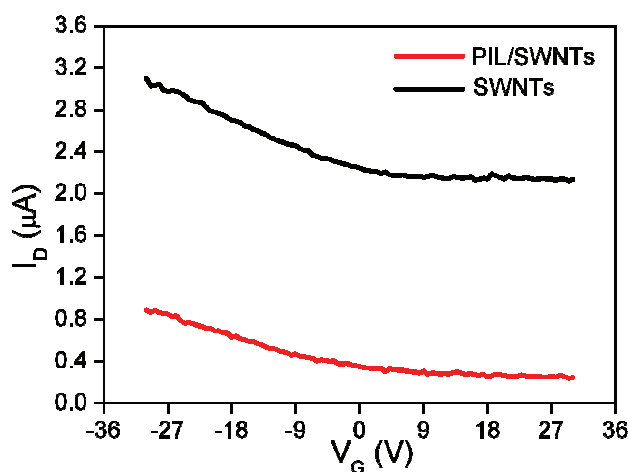


Figure S5 I_{SD} - V_G characteristics of SWNTs and PIL/SWNTs devices.

7. Stability test of CO₂ Sensor

Stability test of our CO₂ sensor is shown in Figure S6, where the sensor response to 1 ppm CO₂ in day 1 and after one month storage in N₂ filled box was compared. It can be seen that there is no considerable change in response signal, indicating the good stability of our CO₂ sensor.

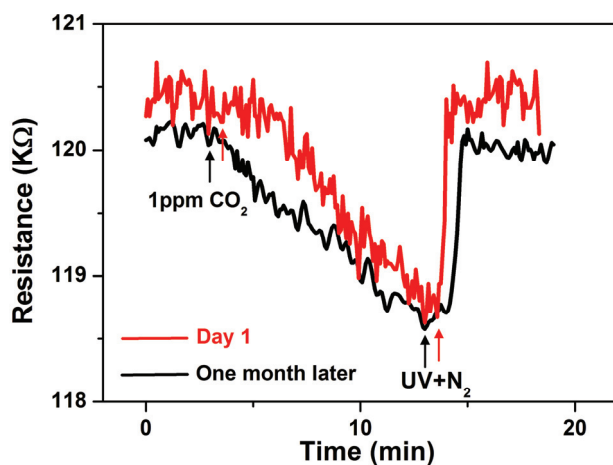


Figure S6 Stability of sensor response to 1 ppm CO₂ in day 1 and after one month.

References:

1. J. B. Tang, H. D. Tang, W. L. Sun, M. Radosz, and Y. Q. Shen, *J. Polym. Sci. Part a-Polym. Chem.*, 2005, **43**, 5477-5489.
2. Tang, J. B.; Tang, H. D.; Sun, W. L.; Radosz, M.; Shen, Y. Q. *J. Polym. Sci. Part a-Polym. Chem.* **2005**, *43*, 5477-5478.
3. S. Mubeen, T. Zhang, B. Yoo, M. A. Deshusses, and N. V. Myung, *J. Phys. Chem. C*, 2007, **111**, 6321-6327.